

# Validation and Calibration of Canada-Wide Coarse-Resolution Satellite Burned-Area Maps

R.H. Fraser,<sup>†</sup> R.J. Hall,<sup>†</sup> R. Landry,<sup>†</sup> T. Lynham, D. Raymond, B. Lee, and Z. Li

## Abstract

*Satellite-based mapping can provide a timely and efficient means of identifying burned vegetation at continental scales for estimating greenhouse gas emissions and impacts on the terrestrial carbon budget. In this study, we used a sample of 55 Landsat Thematic Mapper (TM) scenes distributed across Canada to validate and calibrate 1998 and 1999 national-level burned areas maps produced using coarse resolution (approx. 1-km) SPOT VEGETATION and NOAA AVHRR imagery. Commission and omissions errors, based on fire events greater than 200 ha, were found to be small in the coarse resolution maps (4 percent and 1 percent, respectively). However, the coarse resolution burned-area estimates were 72 percent larger than the crown fire burned area mapped at 30 m using Landsat TM (11,039 versus 6,403 ha average area). This bias was attributed to spatial aggregation effects in which the coarse resolution product included the tree crown fire, partial burn, and unburned fractions of a pixel. A regression calibration model ( $R^2 = 0.95$ ,  $p < 0.0005$ ,  $RMSE = 3,015$  ha,  $n = 155$ ) based on a VGT/TM double sampling approach was derived to correct for the aggregation bias and to provide Canada-wide estimates of crown fire burned area.*

## Introduction

Wildfires are a major source of disturbance to the boreal forest ecosystem because they have been documented as burning as much as 1.5 percent (22 million ha) of its global area in a single year (Cofer *et al.*, 1996). Fires in this ecosystem typically kill the standing trees and thus exert a dominant control on landscape-level patterns of forest succession and stand-age distribution (Johnson, 1992). Fire is an important factor modifying the carbon budget within the boreal zone, which covers less than 17 percent of the Earth's surface area yet accounts for more than 30 percent of its terrestrial carbon storage

(Kasischke, 2000). Carbon storage is directly modified by fire owing to the combustion of canopy and surface layer biomass into atmospheric carbon (e.g., CO<sub>2</sub>, CH<sub>4</sub>, CO). Carbon storage is also indirectly modified due to shifts in stand-age distribution and increased ground-layer decomposition rates following fire (Kasischke, 2000). To assess these ecological and carbon budget impacts, a fundamental parameter that must be measured is burned area. This requires methods to map the spatial distribution of burned forest over vast, remote areas in an accurate, consistent, and timely manner.

Forest fire management in Canada is the responsibility of provincial, territorial, and federal fire management agencies. As such, they are the primary producers of fire databases, including end-of-year burned-area surveys. Depending on the agency, burned area maps are produced using a variety of methods, including aerial photointerpretation, aerial GPS, ground GPS, and interpretation of medium resolution (30-m) Landsat TM imagery. These maps have recently been compiled by the Canadian Forest Service to produce a fire database in GIS format, which includes more than 5,000 fires larger than 2 km<sup>2</sup> that occurred between 1980 and 1995 (Stocks *et al.*, 2002).

Coarse-resolution (approx. 1-km) satellite sensors, notably the Advanced Very High Resolution Radiometer (AVHRR) aboard the NOAA polar orbiters, have proven to be effective for mapping the regional and continental extent of burned areas after fire (Cahoon *et al.*, 1994; Kasischke and French, 1995; Fernandez *et al.*, 1997; Eva and Lambin, 1998a; Barbosa *et al.*, 1999; Fraser *et al.*, 2000a). Such sensors are well suited for mapping boreal fires because more than 97 percent of the burned area in Canada between 1989 and 1998 was caused by fire events greater than 10 km<sup>2</sup> (CCFM, 2003), a size that is significantly larger than the sensor resolution. Furthermore, most burning involves crown fires that destroy the forest canopy, producing a large and immediate change in reflectance that can be easily identified. Although the detail and accuracy of coarse resolution satellite products are generally not sufficient for application to local resource management, they may complement existing conventional burned-area surveys in several ways: (1) they can provide rapid and inexpensive end-of-year burned-area assessment at continental scales; (2) the products are produced using a consistent methodology where area biases should be relatively stable and can be quantified; (3) maps can be produced for remote regions where burning is not extensively monitored, including large tracts of Asian forest (Shvidenko and Nilsson, 2000); and (4) the digital products are compatible for large-scale, spatially explicit modeling of carbon budget and fire emissions within a GIS environment.

<sup>†</sup>Major authors listed in alphabetical order.

R.H. Fraser, R. Landry, and Z. Li are with Natural Resources Canada, Canada Centre for Remote Sensing, 588 Booth St., Ottawa, Ontario K1A-0Y7, Canada (robert.fraser@ccrs.nrcan.gc.ca).

Z. Li is presently with the University of Maryland, Earth System Science Interdisciplinary Center, 2335 CSS Building, College Park, MD 20742-2465.

R.J. Hall and B. Lee are with the Canadian Forest Service, Natural Resources Canada, 5320-122 St., Edmonton, Alberta T6H-3S5, Canada.

T. Lynham is with the Canadian Forest Service, Natural Resources Canada, 1219 Queen Street East, 490, Sault Ste. Marie, Ontario P6A-5M7, Canada.

D. Raymond is with Dendron Resource Surveys Inc., 880 Lady Ellen Place, Suite 206, Ottawa, Ontario, K1Z-5L9, Canada.

Photogrammetric Engineering & Remote Sensing  
Vol. 70, No. 4, April 2004, pp. 451-460.

0099-1112/04/7004-0451/\$3.00/0  
© 2004 American Society for Photogrammetry  
and Remote Sensing

For satellite-based burned-area mapping at continental scales to be more robust, accurate, and widely adopted, two important issues must be addressed. First, the burned-area products must be validated using the best available benchmark, typically a conventional map product if available (Kasischke and French, 1995; Fernandez *et al.*, 1997; Fraser *et al.*, 2000a) or a product based on higher resolution satellite imagery, such as that from Landsat TM (Eva and Lambin, 1998a; Barbosa *et al.*, 1999). Second, any systematic bias in satellite burned-area estimation must be identified and accounted for through calibration or other means. When mapping burned area (or land cover more generally) using coarse resolution sensors, area estimates will normally be biased in landscapes where land-cover types occur at a spatial frequency that is finer than the satellite image resolution. The resulting aggregation effect typically causes the area of more common land-cover classes to be overestimated and the area of less common classes to be underestimated (Moody and Woodcock, 1996). In burned-area mapping, an overestimation, or positive bias, is likely to occur in cases where burns extending over several pixels contain numerous sub-pixel unburned patches (French *et al.*, 1996; Eva and Lambin, 1998b).

Several techniques have been employed to calibrate land-cover proportions from coarse resolution satellite imagery using higher resolution reference data. One strategy involves examining the relationship between coarse resolution *reflectance* and sub-pixel land-cover proportions based on a finer scale classification, such as one from Landsat TM. The translation can be achieved using a variety of methods, including linear mixture modeling (Razafimpanilo *et al.*, 1995; DeFries *et al.*, 2000), artificial neural networks (Foody *et al.*, 1996; Moody *et al.*, 1996), regression (Iverson *et al.*, 1994; DeFries *et al.*, 1997), and labeling of coarse resolution spectral clusters (Fernandes *et al.*, in press). A necessary assumption required to apply these approaches for calibrating burned area is that the spectral signature of the burned forest end member is stable. However, this assumption would be violated for a large-area sample measured at the end of a fire season, because individual fires will have had varying regeneration periods and thus be located at different points along the post-fire spectral trajectory curve (Pereira *et al.*, 1999; Fraser *et al.*, 2000b). Application of unmixing techniques in boreal burns would be further confounded by variation in burn severity (Michalek *et al.*, 2000), fuel type, and background reflectance. A second calibration strategy involves determining the relationship between a *classified* coarse resolution map and sub-pixel cover proportions from a higher resolution classification (Roesch *et al.*, 1995; Mayaux and Lambin, 1997; Eva and Lambin, 1998b), potentially with the addition of auxiliary explanatory variables (Mayaux and Lambin, 1997). We adopted this second approach for calibrating aggregation bias present in coarse resolution burned area maps.

The objective of this study was to address the validation and aggregation issues associated with coarse resolution burned area mapping as they relate to an application of SPOT VEGETATION (VGT) imagery for Canada-wide analysis of burned forest area. This involved three major components:

- Annual mapping of forest burned across Canada in 1998 and 1999 using coarse resolution VGT imagery,
- Mapping a representative sample of these burns using higher resolution Landsat TM imagery, and
- Comparing the coarse and medium resolution burned area estimates from this double sampling approach to conduct a validation and statistical calibration of the coarse resolution product.

## Methods

### Selection of Sample Fires

The first requirement for developing a calibration function to correct coarse resolution burned area is to identify those factors measurable at a national scale that influence the degree of aggregation bias. Four factors that may affect accuracy and bias in the VGT product include fire behavior conditions, burn size, vegetation fuel type, and the level of fragmentation within a burn. Fire behavior will influence burn severity and fuel consumption within a burn, yet this variable has not yet been adequately quantified from coarse resolution satellite data. We did not pursue information related to local fire behavior conditions because obtaining such information is impractical for large area mapping.

Burn size is an important consideration for satellite mapping, because burns larger than the sensor resolution will have a greater likelihood of being detected than will smaller fires. Considering the modulation transfer function and predicted multitemporal registration accuracy of VGT, the effective resolution provided by VGT composited imagery for change detection is about 2 to 3 km (a 4- to 9-km<sup>2</sup> area). Edge effects from fire boundary pixels is an associated issue but may not cause systematic bias because pixels approximately less than half-burned will likely be mapped as unburned, while those more than half burned will be mapped as completely burned. The effect of burn size on the calibration relationship was addressed by sampling a range of fire sizes across Canada.

Forest fuel types in Canada are classified qualitatively based on stand structure and composition (i.e., tree species, vegetation density, and age), surface and ladder fuels, and the forest floor as it relates to the organic soil layer (FCFDG, 1992). In an attempt to obtain a wide range of fuel types in the sampling design, a map of annual fire locations from daily AVHRR imagery (Li *et al.*, 2000) was overlaid with maps of land cover derived from AVHRR (Cihlar and Beaubien, 1999) and terrestrial ecozones of Canada (Figure 1 inset; ESWG, 1996). The intersection of land cover and ecozone with available cloud-free, post-fire TM scenes guided the selection of 55 Landsat TM scenes across Canada (Figure 1).

The degree of burn fragmentation and the scale at which it occurs will likely influence the relationship between SPOT VGT and Landsat TM burned area. For example, if a burn is fragmented at a spatial scale smaller than the effective VGT resolution, overestimation of burned area will occur, assuming that enough of the VGT pixel has burned to be mapped as such (Eva and Lambin, 1998b). As degree of fragmentation increases, the bias increases because a VGT classification will aggregate the unburned patches with a 1-km pixel as burned. To test the hypothesis that the relationship between coarse and fine resolution burned area (i.e., aggregation bias) varies with degree of burn fragmentation (e.g., Mayaux and Lambin, 1997), two fragmentation metrics were computed for each burn from the coarse resolution imagery. A spatial measure of fragmentation was provided using the ratio of interior unburned islands area to the mapped burned area. Fragmentation was also measured in the spectral domain based on the standard deviation of post-fire VGT vegetation index values within each fire.

A basic assumption for applying the coarse resolution fragmentation metrics to calibrate burned area is that they are related (i.e., scale) to the "true" level of fragmentation measured at the Landsat TM scale (Mayaux and Lambin, 1997). We tested this requirement for the sample fires by examining the correlation between the coarse scale metrics and degree of fragmentation measured in the TM maps. "True" fragmentation was measured using the ratio of TM-mapped burned area to

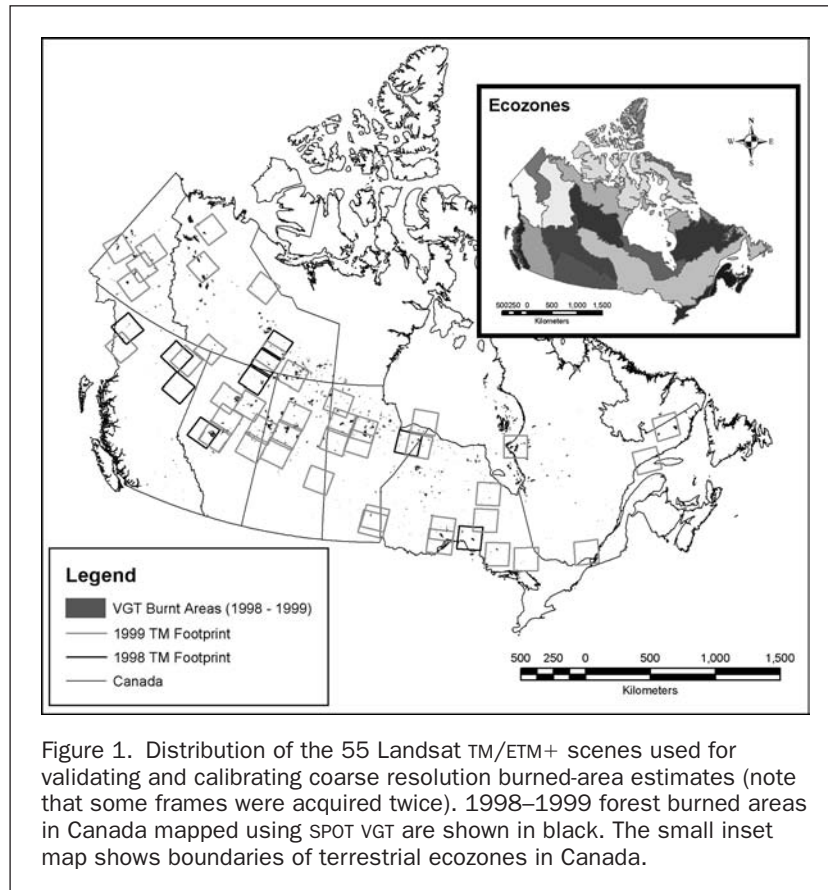


Figure 1. Distribution of the 55 Landsat TM/ETM+ scenes used for validating and calibrating coarse resolution burned-area estimates (note that some frames were acquired twice). 1998–1999 forest burned areas in Canada mapped using SPOT VGT are shown in black. The small inset map shows boundaries of terrestrial ecozones in Canada.

the area contained within a generalized TM burn perimeter that encloses all interior unburned islands. Generalized outer perimeters were created by expanding and contracting the TM burn polygons by 200 m, then eliminating any interior polygons. TM-level fragmentation was also measured from the total length of the burn/non-burn edge lying interior and exterior of a burn. Edge length was divided by the square root of the burned area to make the metric insensitive to burn size (such an edge metric was not used to measure VGT fragmentation because, at a 1-km scale, it was largely related to burn perimeter complexity as determined by fire size).

Burn size, vegetation fuel type, ecozone, and VGT-measured fragmentation within each burn were therefore incorporated into a sample design to select burns for statistical analysis and calibration, because these auxiliary variables could be readily quantified at a national scale using coarse resolution imagery.

#### National-Scale Coarse Resolution Burned-Area Mapping Using SPOT VGT

Mapping of burned forest across Canada for 1998 and 1999 was performed using a technique developed for annual, coarse resolution mapping of burned boreal forest canopy presented in Fraser *et al.* (2000a). The hybrid method, dubbed Hotspot and NDVI Differencing Synergy (HANDS), combines active fire monitoring with multitemporal change detection. Change detection and identification of new burned areas is accomplished by differencing a pair of post-fire season vegetation indices derived from anniversary date composited imagery. A cumulative mask representing the locations of actively burning fires, detected with daily satellite imagery, is first used to derive regional-level (i.e., 200 km by 200 km) difference thresholds, followed by more restrictive, locally adaptive thresholds. The local thresholds are computed for individual burn patches, which are isolated by spatially

clumping all potentially burned pixels identified using the regional threshold.

In this study, annual masks of 1998 and 1999 fire locations were created by compositing daily fire masks produced from NOAA/AVHRR imagery (Li *et al.*, 2000) as part of the Fire M3 project (<http://fms.nofc.cfs.nrcan.gc.ca/FireM3/>, last accessed 25 December 2003). The differencing component of HANDS was accomplished using a vegetation index (VI) derived from SPOT VGT that provides optimal discrimination of burned boreal forest based on the normalized difference between NIR and SWIR reflectance (Fraser *et al.*, 2000b). The VI was computed from cloud free, 30-day VGT composites that were corrected for atmospheric, bidirectional reflectance distribution function (BRDF), and cloud contamination effects (Cihlar *et al.*, 1997). The 1999 burned-area mapping involved differencing of September 1998 and 1999 post-fire season composites. For 1998 mapping, differencing was performed on composite Vis from May 1998 and September 1998 (VGT became operational in April 1998, precluding the use of an anniversary date composite from September, 1997).

#### Medium Resolution Burned-Area Mapping Using Landsat TM

To provide a basis for validating and calibrating the coarse resolution burned-area maps, a sample of 174 burns from 1998–1999 was mapped using 55 Landsat TM/ETM+ scenes (Figure 1). Selection of the cloud-free TM/ETM+ scenes was optimized to reflect the widest possible distribution of Canadian terrestrial ecozones, fuel types, and burn sizes greater than 200 ha, while maximizing the number of burns contained within a scene. This method for scene selection is summarized in Figure 2. The algorithm used for TM/ETM+ burned-area mapping (Figure 3) was designed and tested for use in post-fire timber salvage planning by the forest products

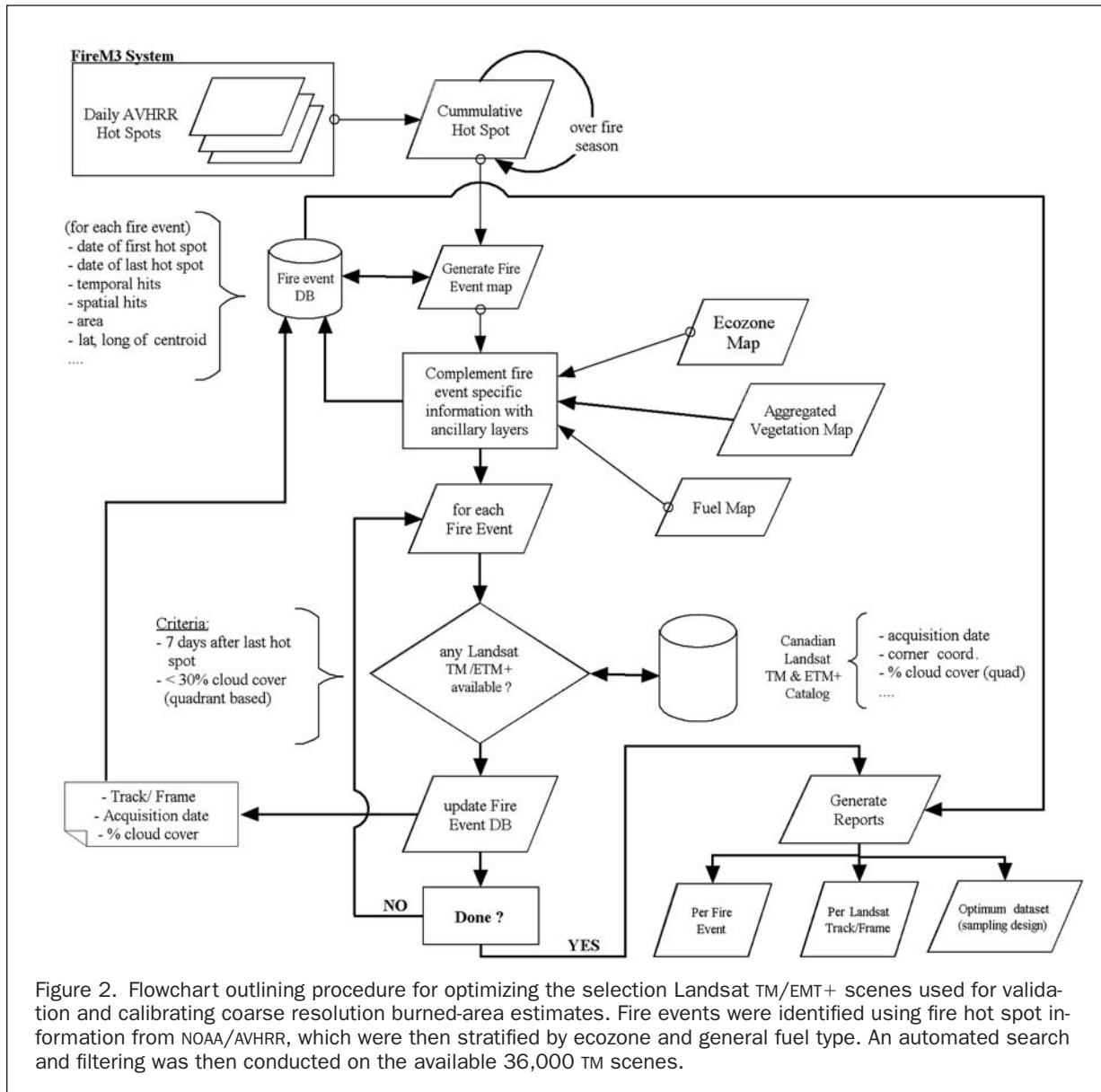


Figure 2. Flowchart outlining procedure for optimizing the selection Landsat TM/ETM+ scenes used for validation and calibrating coarse resolution burned-area estimates. Fire events were identified using fire hot spot information from NOAA/AVHRR, which were then stratified by ecozone and general fuel type. An automated search and filtering was then conducted on the available 36,000 TM scenes.

industry and provincial governments. As such, it was optimized to map forested areas with greater than 50 percent burnt crowns because this represents the highest priority area for salvage logging within forest management practices. Unlike the HANDS technique, the algorithm requires only a single post-burn Landsat TM/ETM+ scene acquired in the same or following year of the fire. Top-of-atmosphere reflectance was computed for all bands and orthorectified to a Universal Transverse Mercator (UTM) coordinate system and resampled to a 25-m resolution. For the validation process, digital elevation data were used during the orthorectification.

Preliminary burned areas were identified using a first approximation statistical threshold applied to a VI from TM that combines the NIR and SWIR channels. Positive false alarms (clouds, water bodies, and recent cuts) were automatically removed during this process. These seed pixels are buffered and clustered into discrete fire events, then each cluster is individually refined based on its unique signature. Spectral reference metrics are then derived for each fire event that become the criteria used to assess a merit class to each polygon from a particular fire event. The metrics are thus designed to be

self-adaptive to local variation in burn reflectance due to varying vegetation cover, time between the fire event and image acquisition, and fire severity among different burns within a Landsat scene.

Validation of the technique was performed over a 60,980-ha burn using 1:20,000-scale color-infrared (CIR) aerial photographs (Plate 1). An independent company was contracted to interpret burned area and severity from the CIR photographs. A complete burn class and six partial burn classes were interpreted by registered photointerpreters from the aerial photographs, and georeferenced vectors were provided for the analysis. The complete burn class and partial burn class for areas greater than 50 percent crown burnt were the only classes used for the validation of the Landsat TM-derived burnt vector product.

The burned area derived using the Landsat TM technique agreed with the CIR maps to within 6 percent for complete burns and areas greater than 50 percent crown burnt. Following provincial fire management agency convention for burned-area mapping, only polygons larger than 2 hectares were retained in the final vector product.

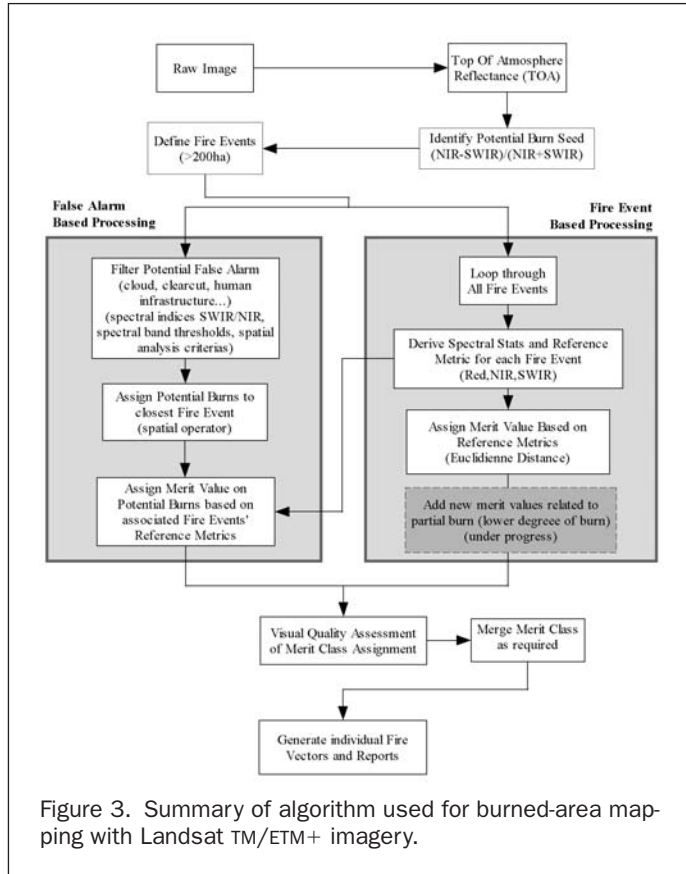


Figure 3. Summary of algorithm used for burned-area mapping with Landsat TM/ETM+ imagery.

### Data Analysis

One method previously used to calibrate the area of binary classes from coarse resolution imagery, including burned area (Eva and Lambin, 1998b) and forest cover (Mayaux and Lambin, 1997), is to sample the coarse and fine resolution mapped areas within rectangular blocks of pixels (e.g., 15 km by 15 km). The statistics computed within each block (e.g., burned area and fragmentation) can then be used as samples to derive an empirical calibration model. Considering the discrete nature and relatively large size of boreal burns (38 km<sup>2</sup> average for the national 1998 and 1999 VGT product) and the availability of precision geocoded imagery, the samples we selected for comparison consisted of the individual burn patches contained within the TM scenes. A burn was defined as a cluster of pixels in the VGT burned-area mask where no pixel is separated by more than 2 km.

Descriptive statistics (e.g., mean, standard deviation, minimum, maximum, coefficient of variation), Pearson's product moment correlation, and scatterplots were used to describe this sample mapped using VGT and TM. Before developing a calibration model, the accuracy of the VGT product was

assessed where it overlaps the TM scenes by comparing the individual burn areas mapped by (1) both sensors; (2) TM but not VGT, representing VGT omission error; and (3) VGT but not TM, representing VGT commission error. A one-way analysis of covariance was conducted to determine if fuel type and terrestrial ecozone were factors influencing burned-area bias in the VGT product. A calibration model was then developed using the sample of fires mapped by both sensors and the auxiliary variables, and applied to the national-level VGT burned-area maps. Both simple and multiple regression analysis were used to develop calibration models to estimate TM burned area (i.e., "true" crown fire-burned area) as a function of VGT burned area and fragmentation. The regression calibrations were evaluated by the adjusted R<sup>2</sup>, root-mean-square error (RMSE), significance of regression coefficients, and residual error plots. All statistical tests in this study were conducted at the 5 percent probability level.

## Results and Discussion

### Comparison of Burned Areas within the Landsat TM Validation Scenes

A total of 174 burns were mapped within the 55 validation scenes using the TM algorithm, representing a crown fire burned area of 1,001,027 ha (5,753 ha mean area). Larger fires were less frequent, with burned area following a negative exponential-shaped distribution. Of these 174 burns, 19 were not mapped by VGT and cover 8,593 ha (452 ha mean area). Thus, based on the TM sample, observed omission error from VGT was 11 percent (19/174) in terms of number of fire events greater than 200 ha, yet was much less significant in terms of extent. Investigating SPOT VGT commission error, there were 128 falsely mapped burns contained within the footprints of the TM scenes. These burns were relatively small, with an average area of 498 ha and totaling 63,700 ha. Commission error was 3.6 percent relative to the VGT-mapped burned area (i.e., 63,700/1,774,710).

Table 1 presents summary statistics for VGT and TM burned area based on the 155 burns mapped by both sensors within the 55 Landsat TM validation scenes. Coarse resolution burned area from VGT for these common burns was 1,711,010 ha (11,039 ha mean area). By comparison, the TM-based crown fire burned area was 992,434 ha, or 42 percent smaller. Plates 2A and 2C show a comparison of the VGT and TM burned-area maps for two sample fires in which the TM burned-area estimates were 47 percent and 35 percent smaller than those from VGT. Examination of the VGT and TM mapped areas in relation to the raw TM imagery and available CIR aerial photographs indicated that this bias was mainly attributable to spatial aggregation effects, where the effective resolution of the composited VGT imagery was not sufficient to identify unburned islands within the outer burn boundaries. This observation was also supported by the close one-to-one relationship between the VGT-mapped burned areas and the areas enclosed by the generalized TM burn perimeters (e.g., Plates 2B and 2D). The average generalized TM area was 10,398 ha, or only 6 percent less than that

TABLE 1. DESCRIPTIVE STATISTICS FOR BURNED AREAS AND FRAGMENTATION METRICS BASED ON 155 COMMON FIRES CONTAINED WITHIN THE 55 LANDSAT TM VALIDATION SCENES

Statistic <sup>1</sup>	VGT Area	TM Area	VGT Spatial	VGT Spectral
Sum	1,711,010	992,434	N/A	N/A
Mean	11,039	6,403	15.8	90.6
Standard Deviation	20,288	11,714	24.7	45.4
Minimum	100	229	0	0
Maximum	133,900	79,975	148	318
Coefficient of Variation	1.84	1.83	1.57	0.5

<sup>1</sup>Units are hectares except for Coefficient of Variation.

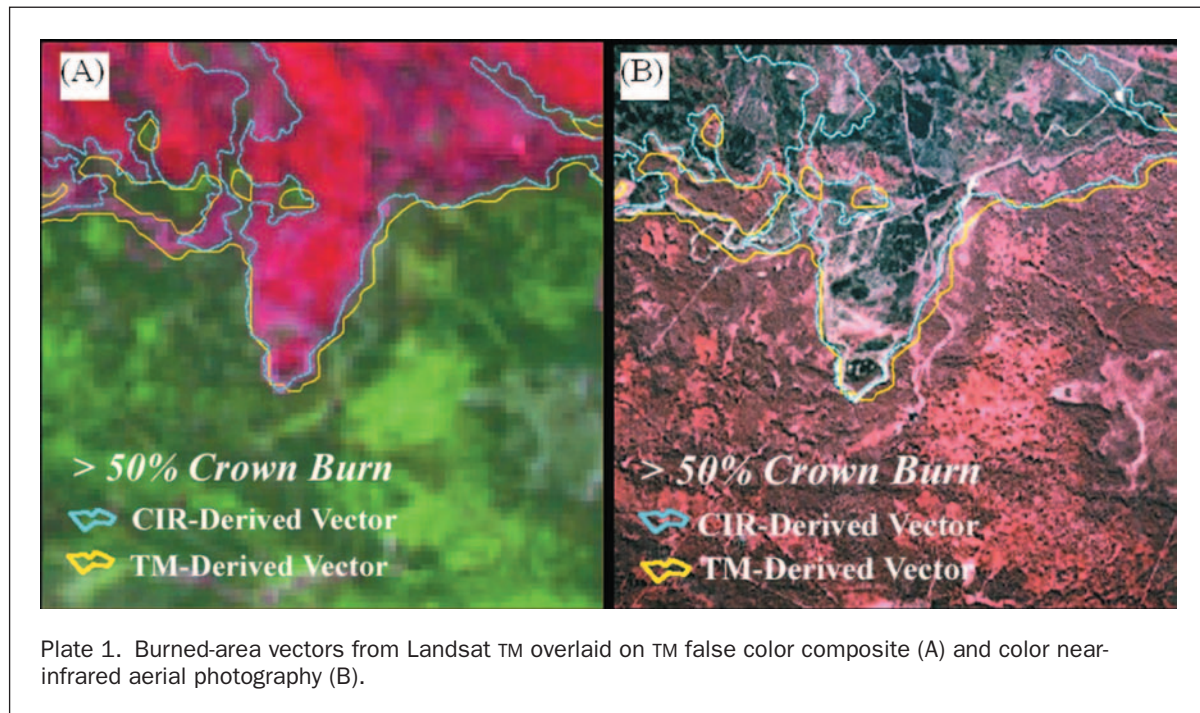


Plate 1. Burned-area vectors from Landsat TM overlaid on TM false color composite (A) and color near-infrared aerial photography (B).

from the VGT burns, while linear regression produced a slope of 0.98 ( $r^2 = 0.96$ ;  $p < 0.0001$ ). The unburned islands mapped as burned by VGT may be composed of non-burned forest or forest subjected mainly to surface fire below the canopy. They may also correspond to non-fuel areas, including open water, spruce wetlands, or barren areas. The portion of bias attributable to water bodies could be quantified using a new 1-km map of Canada-wide water fractions that was derived by aggregating vector data from the National Topographic Data Base (Fernandes *et al.*, 2001). Eight percent of the total 1998–1999 VGT burned area or 18 percent of the VGT bias could be accounted for by sub-pixel surface water content.

The large fraction of interior unburned area contrasts the observations of Eberhart and Woodard (1987), who found that only about 5 percent of burns in Alberta larger than 2,000 ha were composed of unburned islands. This difference could be related to the smaller fire sizes examined in Alberta, because the proportion of unburned island area increases in large fires (Gasaway and DuBois, 1985; Eberhart and Woodard, 1987), which were more common in our sample. The variation in island proportion was likely attributable also to the different definitions of burned area adopted in the two studies. Here, the TM-based algorithm was based on a conservative definition that required greater than 50 percent crown destruction, thereby excluding partially burned areas mapped as burned by Eberhart and Woodard (1987).

Despite the large differences in burned areas mapped using the two sensors, the areas of the individual polygons were strongly correlated ( $r = 0.97$ ,  $p < 0.0001$ ,  $n = 155$ ) and linearly associated (Figure 4). The proportional difference from the two sets of burned-area estimates appeared relatively consistent, which would support the use of linear regression as a means of calibrating the coarse resolution burned areas from SPOT VGT.

#### Deriving a Calibration Model for Coarse Resolution Burned Area

Terrestrial ecozone and forest fuel type were hypothesized to be important in determining the variation in burned areas mapped from the VGT and TM sensors. However, based on a one-way analysis of covariance with burned area as the

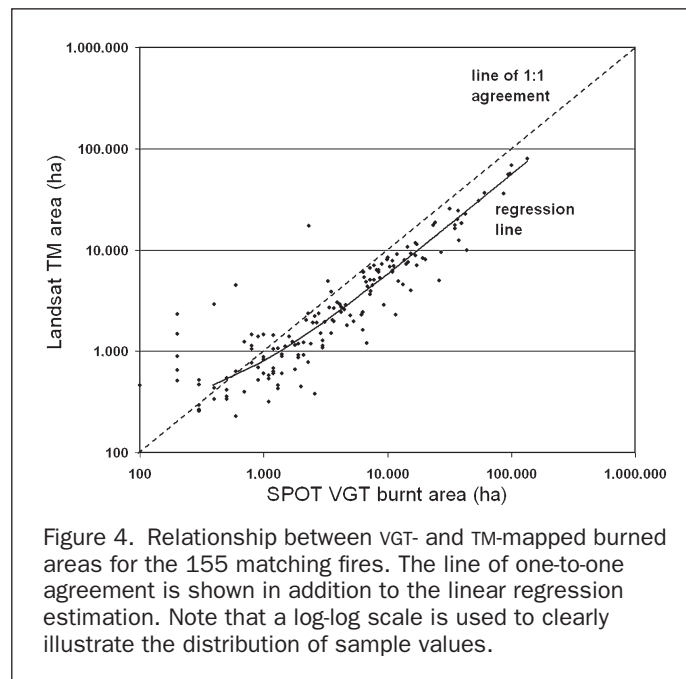


Figure 4. Relationship between VGT- and TM-mapped burned areas for the 155 matching fires. The line of one-to-one agreement is shown in addition to the linear regression estimation. Note that a log-log scale is used to clearly illustrate the distribution of sample values.

response variable and VGT and TM as the factor variable, neither terrestrial ecozone ( $p = 0.501$ ) nor forest fuel type ( $p = 0.77$ ) were significant covariate factors. Most of the burned areas occurred in conifer forest having generally similar fire behavior, and this may explain, in part, why these variables were not statistically important for coarse resolution burned area mapping.

Simple and multiple regression models were developed to predict “true” crown fire burned area derived from TM based on VGT burned area and the spatial and spectral fragmentation indices. The resulting models, summarized in Table 2, indicated that neither fragmentation index was significant in explaining the variation between TM and VGT

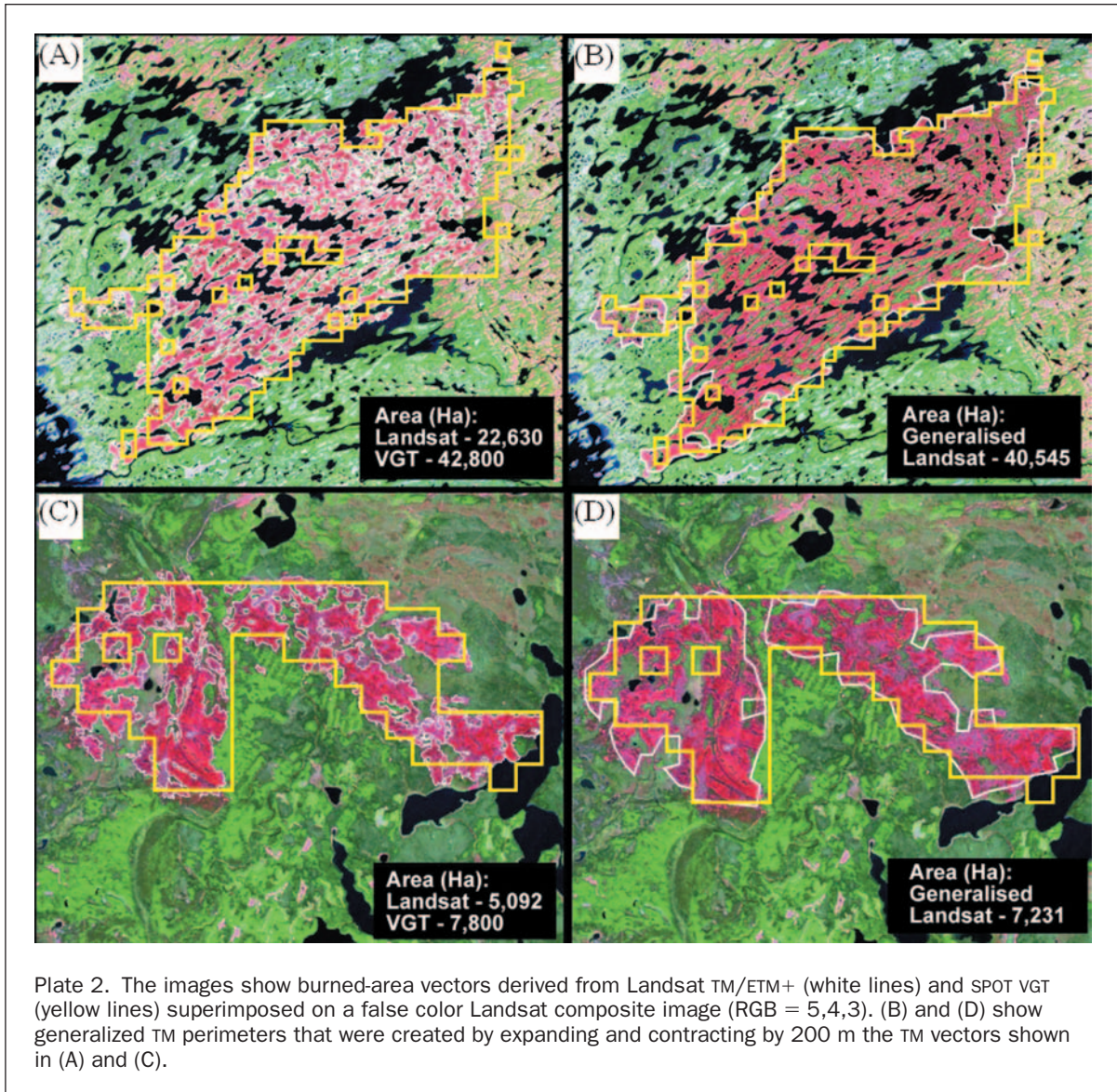


TABLE 2. SUMMARY REGRESSION STATISTICS

Model Form	Regression Parameters			R <sup>2</sup>	SEOE <sup>1</sup> (ha)
	B <sub>0</sub>	B <sub>1</sub>	B <sub>2</sub>		
1. TM area = B <sub>0</sub> + B <sub>1</sub> VGT area	243.06 (p = 0.38)	0.56 (p = 0.00)		0.93	3018
2. TM area = B <sub>0</sub> + B <sub>1</sub> VGT area + B <sub>2</sub> VGT spectral	247.64 (p = 0.65)	0.56 (p = 0.00)	-0.053 (p = 0.99)	0.93	3028
3. TM area = B <sub>0</sub> + B <sub>1</sub> VGT area + B <sub>2</sub> VGT spatial	279.28 (p = 0.35)	0.56 (p = 0.00)	-4.13 (p = 0.72)	0.93	3026
4. TM area = B <sub>0</sub> + B <sub>1</sub> VGT area	0	0.56 (p = 0.00)		0.95	3015

<sup>1</sup>SEOE: Standard error of estimate.

burned area for the 155 matching fires. The major reason for this was that VGT-measured burn fragmentation at 1 km was not an effective proxy for true levels of fragmentation represented in the TM product. VGT spectral fragmentation was not correlated with either the ratio or edge measures of TM frag-

mentation. VGT spatial fragmentation was weakly correlated with the ratio ( $r = -0.45$ ,  $p < 0.0001$ ) and edge ( $r = 0.58$ ,  $p < 0.0001$ ) measures of TM fragmentation, yet its effectiveness is limited by the fact that only 70/155 VGT samples had any interior islands and thus could provide an index of

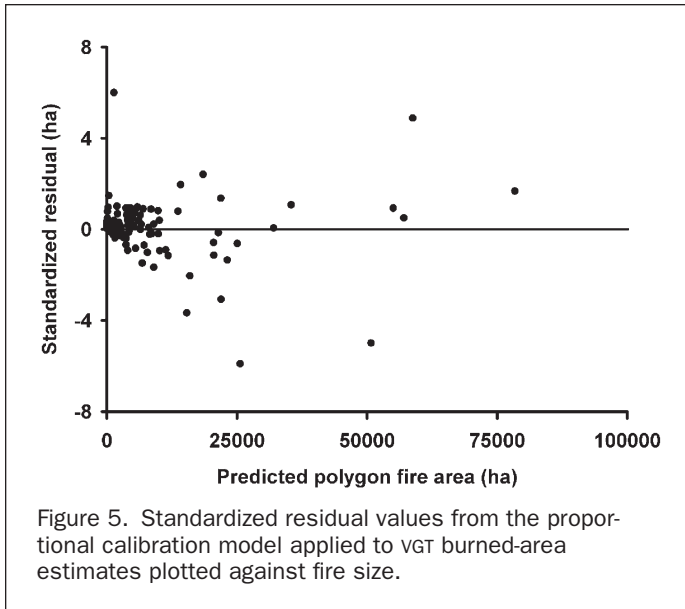


Figure 5. Standardized residual values from the proportional calibration model applied to VGT burned-area estimates plotted against fire size.

spatial fragmentation. Overall, these results suggest that variability in fine-scale fragmentation of boreal burns does not scale up to about 2 to 3 km such that VGT imagery can provide an effective measure of this fragmentation.

The regression analysis indicated that a simple proportional adjustment to VGT burn area is sufficient for calibration, because the regression intercept terms were not statistically significant (Table 2). This proportional model explained almost all of the variation in TM area ( $r^2 = 0.95$ ,  $p < 0.0001$ ), while producing a standard error of estimate of 3,015 ha. The residual plot for the proportional model also appears to be random over the range of the data (Figure 5), indicating that the bias in VGT burn area is relatively consistent over the range of fires examined in this study.

#### National-Level Burned Area and Application of Calibration Function

Figure 1 presents the 1-km national-level burned area maps from 1998–1999 produced using the HANDS algorithm. The first data column in Table 3 lists burned area by Canadian province/territory for 1998 and 1999 based on official statistics produced by fire management agencies and compiled by the Canadian Interagency Forest Fire Centre (CIFFC) ([www.cifffc.ca](http://www.cifffc.ca), data last accessed 25 December 2003; CIFFC, 1998; CIFFC, 1999). These figures are typically based on surveys from GPS or photointerpretation and consider both

surface and crown fire affected areas. The level of detail provided by the surveys varies, with most identifying large unburned green islands and some identifying smaller islands as well. Column 2 lists the corresponding 1998 and 1999 province and national level burned areas derived using the HANDS technique applied to VGT and AVHRR imagery. For most provinces/territories, uncalibrated satellite burned areas were similar to conventional estimates, while Canada-wide burned area was within 15 percent of the CIFFC-compiled burned area for both years. These results are comparable to those obtained for 1995 and 1996 Canada-wide mapping in Fraser *et al.* (2000a) using AVHRR, where a strong correlation between the areas of 276 burns in five provinces was demonstrated. In general, the coarse resolution imagery produces burned-area estimates similar to those based on conventional mapping methods. While VGT imagery will be sensitive mainly to reflectance changes from crown destruction, its limited resolution leads to surface burns and smaller unburned islands being mapped as burned, similar to most of the conventional products.

The third column in Table 3 shows provincial- and national-level burned areas after applying the TM-based regression calibration function to the coarse resolution burned-area maps. Considering the design of the TM algorithm, these calibrated areas represent forest canopy that was nearly completely burned by crown fire, and exclude lightly burned areas (surface fires where tree crown remains largely intact) and unburned green islands within the burns. This Canada-wide crown fire area is, as expected, significantly smaller than both the conventional CIFFC burned area (by 52 percent and 38 percent) and VGT-based burned area (by 44 percent both years). Note that, because the fire-specific auxiliary variables (fragmentation and fuel type) were not significant in the statistical models, the calibration does not provide a spatially variable estimate of VGT aggregation bias. However, the strong correlation ( $r = 0.97$ ) between the TM and VGT burned areas indicates that the bias is reasonably stable.

The calibrated estimates of crown fire burned area from VGT can complement existing conventional burned-area estimates by partitioning the average crown fire burned-area fraction from the total area contained within the outer burn perimeter. This information could provide a useful input for predicting continental-scale forest fire emissions, because crown fires indicate a more intense fire (Van Wagner, 1976) with corresponding greater fuel consumption (Stocks, 1989; Stocks and Kauffman, 1997) and release of carbon emissions (Conard and Ivanova, 1997). For example, in Ontario mature jack pine forests subject to low intensity or vigorous surface fires ( $n = 10$ ), total fuel consumption averaged 1.06 kg/m<sup>2</sup>, while those that underwent crowning ( $n = 2$ ) had an average

TABLE 3. BURNED AREA (HA) BY PROVINCE/TERRITORY FOR 1998 AND 1999

Province	Fire Management Agency ('98/'99)	SPOT VGT/HANDS ('98/'99)	SPOT VGT Calibrated ('98/'99)
NWT	1,459,360/550,046	1,274,500/506,400	713,720/283,584
Saskatchewan	995,498/180,820	792,300/181,500	443,688/101,640
Alberta	734,816/122,612	542,400/132,700	303,744/74,312
Quebec	418,318/97,747	421,600/125,800	236,096/70,448
Manitoba	408,918/121,826	457,500/325,600	256,200/182,336
Yukon	385,579/185,956	294,400/159,900	164,864/89,544
Ontario	158,218/328,248	209,700/421,000	117,432/235,760
British Columbia	77,781/10,620	79,800/15,000	44,688/8,400
Newfoundland	40,226/39,292	2,500/30,300	1,400/16,968
Nova Scotia	397/1,822	0/2,300	0/1,288
N. Brunswick	303/1,211	0/800	0/448
PEI	77/77	0/0	0/0
Total	4,710,775/1,705,645	4,074,700/1,901,300	2,281,832/1,064,728

consumption of 1.75 kg/m<sup>2</sup> (Stocks, 1989). Most previous estimates of continental-scale boreal fire emissions have multiplied burned area, as calculated from conventional or coarse resolution satellite mapping, by a fuel consumption factor that was measured in experimental crown fires. Because this approach assumes that all burned area is represented by crown fire, it may overestimate the release of carbon to the atmosphere.

One limitation with the calibrated burned-area estimates is that they cannot distinguish between partially (less than 50 percent) and completely unburned areas of the residual non-crown fire component. A valuable extension to this study would be to develop a TM-based procedure for separating the partially burned crown fire areas from unburned areas and surface fires. This would allow explicit partitioning of unburned green islands from the coarse resolution burned-area estimates for carbon budget and ecological studies.

## Summary and Conclusions

The purpose of this study was to apply medium resolution Landsat TM imagery for validating and calibrating burned-area products produced using coarse resolution VGT and AVHRR imagery. Our major findings and conclusions are as follows:

- National- and regional-scale forest burned-area estimates derived from coarse resolution imagery were comparable to conventional burned-area estimates from GPS and aerial photointerpretation. Composited VGT imagery was able to capture the distribution of large burns (greater than 10 km<sup>2</sup>), which account for most burning in the boreal zone.
- A spatially explicit validation of the VGT burned-area product based on a sample of 174 burns within 55 Landsat TM scenes indicated that VGT is able to effectively map the occurrence and dimension of individual burns with low levels of omission and commission error.
- VGT burned areas were, on average, 72 percent larger than crown fire burned areas mapped using Landsat TM. This bias was caused by spatial aggregation effects where the effective resolution provided by VGT imagery was insufficient to distinguish unburned islands and partially burned areas from the crown fire burned areas contained within a burn. Such a bias could result in overestimating carbon emissions from boreal fires if it is assumed that all burning leads to complete crown destruction.
- A simple linear regression calibration model based on a VGT/TM double sampling approach was effective in removing the coarse resolution bias. Potential, spatially variable predictors of the bias (fuel type, ecozone, burn fragmentation) were not found to be helpful in the model, implying that it is suitable only for providing an aggregate correction factor.
- Further development of the TM-based mapping algorithm to identify partially burned areas could help partition coarse-scale burned area estimates into crown fire, partial burning, and interior unburned fractions.

## Acknowledgments

We would like to acknowledge the significant contributions made in data processing by Heather McLeod and J.-F. Saulnier from the Canada Centre for Remote Sensing. This project received funding from NRCan On Line, Natural Resources Canada's knowledge management initiative (formerly ResSources).

## References

Barbosa, P.M., J.M. Gregoire, and J.M.C. Pereira, 1999. An algorithm for extracting burned areas from time series of AVHRR GAC data applied at a continental scale, *Remote Sensing of Environment*, 69:253–263.

Cahoon, D.R., B.J. Stocks, J.S. Levine, W.R. Cofer, and J.M. Pierson, 1994. Satellite analysis of the severe 1987 forest fires in northern China and southeastern Siberia, *Journal of Geophysical Research*, 99:18,627–18,638.

CCFM, 2003. *National Forestry Database Program*, Canadian Council of Forest Ministers, Canadian Forest Service, Natural Resources Canada, <http://nfdp.ccfm.org/>, last accessed 25 December 2003.

CIFFC, 1998. *Canada Report 1998*, Canadian Interagency Forest Fire Centre, Winnipeg, Manitoba, Canada, 8 p.

———. 1999. *Canada Report 1999*, Canadian Interagency Forest Fire Centre, Winnipeg, Manitoba, Canada, 8 p.

Cihlar, J., H. Ly, Z. Li, J. Chen, H. Pokrant, and F. Huang, 1997. Multi-temporal, multichannel AVHRR data sets for land biosphere studies: Artifacts and corrections, *Remote Sensing of Environment*, 60:35–57.

Cihlar, J., and J. Beaubien, 1999. *Land Cover of Canada Version 1.1., Special Publication, NBIOME Project*, produced by the Canada Centre for Remote Sensing and the Canadian Forest Service, Natural Resources Canada (available on CD-ROM from the Canada Center for Remote Sensing, Ottawa, Ontario, Canada; also available at [ftp://ftp2.ccrs.nrcan.gc.ca/ftp/ftp/ad/EMS/landcover95/Lc95doc1\\_1.txt](ftp://ftp2.ccrs.nrcan.gc.ca/ftp/ftp/ad/EMS/landcover95/Lc95doc1_1.txt), last accessed 30 December 2003).

Cofer, W.R., E.L. Winstead, B.J. Stocks, L.W. Overbay, J.G. Goldammer, D.R. Cahoon, and J.S. Levine, 1996. Emissions from boreal forest fires: Are the atmospheric impacts underestimated?, *Biomass Burning and Global Change* (J.S. Levine, editor), MIT Press, Cambridge, Massachusetts, pp. 834–839.

Conrad, S.G., and G.A. Ivanova, 1997. Wildfire in Russian boreal forests—Potential impacts of fire regime characteristics on emissions and global carbon balance estimates, *Environmental Pollution*, 98:305–313.

DeFries, R., M. Hansen, M. Steininger, R. Dubayah, R. Sohlberg, and J. Townshend, 1997. Subpixel forest cover in Central Africa from multi-sensor, multi-temporal data, *Remote Sensing of Environment*, 60:228–246.

DeFries, R.S., M.C. Hansen, and J.R. Townshend, 2000. Global continuous fields of vegetation characteristics: a linear mixture model applied to multi-year 8 km AVHRR data, *International Journal of Remote Sensing*, 21:1389–1414.

Eberhart, K.E., and P.M. Woodard, 1987. Distribution of residual vegetation associated with large fires in Alberta, *Canadian Journal of Forestry Research*, 17:1207–1212.

ESWG, 1996. *A National Ecological Framework for Canada*, Ecological Stratification Working Group, Agriculture and Agri-Food Canada, Research Branch, Centre for Land and Biological Resources Research and Environment Canada, State of Environment Directorate, Ottawa, Ontario, Canada, 125 p.

Eva, H., and E.F. Lambin, 1998a. Burnt area mapping in Central Africa using ATSR data, *International Journal of Remote Sensing*, 19:3473–3497.

———. 1998b. Remote sensing of biomass burning in tropical regions: Sampling issues and multisensor approach, *Remote Sensing of Environment*, 64:292–315.

Fernandes, R.A., G. Pavlic, W. Chen, and R. Fraser, 2001. *Canada-Wide 1-km Water Fraction Derived from National Topographic Data Base Maps*, Natural Resources Canada, URL: <http://www.geogratis.ca>, last accessed 25 December 2003.

Fernandes, R., R. Fraser, R. Latifovic, J. Cihlar, J. Beaubien, and Y. Du, in press. Approaches to fractional land cover and continuous field mapping: A comparative assessment over the BOREAS study region, *Remote Sensing of Environment*, in press.

Fernandez, A., P. Illera, and J.L. Casanova, 1997. Automatic mapping of surfaces affected by forest fires in Spain using AVHRR NDVI composite image data, *Remote Sensing of Environment*, 60:153–162.

Foody, G.M., R.M. Lucas, P.J. Curran, and M. Honzak, 1996. Estimation of the areal extent of land cover classes that occur at a sub-pixel level, *Canadian Journal of Remote Sensing*, 22:428–432.

FCFDG, 1992. Development and structure of the Canadian forest fire behavior prediction system, Forestry Canada Fire Danger Group, Inf. Rep. ST-X-3, Forestry Canada, Science and Sustainable Development Directorate, Ottawa, Ontario, Canada, 63 p. + photos.

Fraser, R.H., Z. Li, and J. Cihlar, 2000a. Hotspot and NDVI Differencing Synergy (HANDS): A new technique for burned area mapping over boreal forest, *Remote Sensing of Environment*, 74:362–376.

- Fraser, R.H., Z. Li, and R. Landry, 2000b. SPOT VEGETATION for characterizing boreal forest fires, *International Journal of Remote Sensing*, 21:3525–3532.
- French, N.H.F., E.S. Kasischke, R.D. Johnson, L.L. Bourgeau-Chavez, A.L. Frick, and S. Ustin, 1996. Estimating fire-related carbon flux in Alaskan boreal forests using multisensor remote sensing data, *Biomass Burning and Global Change* (J.S. Levine, editor), MIT Press, Cambridge, Massachusetts, pp. 808–826.
- Gasaway, W.C., and S.D. DuBois, 1985. Initial response of moose, Alces alces, to a wildfire in interior Alaska, *Canadian Field-Naturalist*, 99:135–140.
- Iverson, L.R., E.A. Cook, and R.L. Graham, 1994. Regional forest cover estimation via remote sensing: The calibration center concept, *Landscape Ecology*, 9:159–174.
- Johnson, E.A., 1992. *Fire and Vegetation Dynamics: Studies from the North American Boreal Forest*, Cambridge University Press, Cambridge, United Kingdom, 143 p.
- Kasischke, E.S., 2000. Boreal ecosystems in the global carbon cycle, *Fire, Climate Change and Carbon Cycling in the Boreal Forest* (E.S. Kasischke and B.J. Stocks, editors), Ecological Studies Series, Springer-Verlag, New York, N.Y., pp. 19–30.
- Kasischke, E.S., and N.H. French, 1995. Locating and estimating the areal extent of wildfires in Alaskan boreal forests using multiple-season AVHRR NDVI composite data, *Remote Sensing of Environment*, 51:263–275.
- Li, Z., S. Nadon, and J. Cihlar, 2000. Satellite detection of Canadian boreal forest fires: Development and application of an algorithm, *International Journal of Remote Sensing*, 21:3057–3069.
- Mayaux, P., and E.F. Lambin, 1997. Tropical forest area measured from global land cover classifications: Inverse calibration models based on spatial textures, *Remote Sensing of Environment*, 59:29–43.
- Michalek, J.L., N.H.F. French, E.S. Kasischke, R.D. Johnson, and J.E. Colwell, 2000. Using Landsat TM data to estimate carbon release from burned biomass in an Alaskan spruce forest complex, *International Journal of Remote Sensing*, 21:323–338.
- Moody, A., and C.E. Woodcock, 1996. Calibration-based models for correction of area estimates derived from coarse resolution land-cover data, *Remote Sensing of Environment*, 58:225–241.
- Moody, A., S. Gopal, and A.H. Strahler, 1996. Artificial neural network response to mixed pixels in coarse-resolution satellite data, *Remote Sensing of Environment*, 58:329–343.
- Pereira, J.M.C., A.C.L. Sa, A.M.O. Sousa, J.M.N. Silva, T.N. Santos, and J.M.B. Carreiras, 1999. Spectral characterisation and discrimination of burnt areas, *Remote Sensing of Large Wildfires* (E. Chuvieco, editor), Springer-Verlag, Berlin, Germany, pp. 123–138.
- Razafimpanilo, H., R. Frouin, S.F. Iacobellis, and R.C.J. Somerville, 1995. Methodology for estimating burned area from AVHRR reflectance data, *Remote Sensing of Environment*, 54:273–289.
- Roesch, F.A., P.C. Van Deusen, and Z. Zhu, 1995. A comparison of various estimators for updating forest area coverage using AVHRR and forest inventory data, *Photogrammetric Engineering & Remote Sensing*, 61:307–311.
- Shvidenko, A.Z., and S. Nilsson, 2000. Extent, distribution, and ecological role of fire in Russian forests, *Fire, Climate Change and Carbon Cycling in the Boreal Forest* (E.S. Kasischke and B.J. Stocks, editors), Ecological Studies Series, Springer-Verlag, New York, N.Y., pp. 132–150.
- Stocks, B.J., 1989. Fire behavior in mature jack pine, *Canadian Journal of Forestry Research*, 19:783–790.
- Stocks, B.J., and J.B. Kauffman, 1997. Biomass consumption and behavior of wildland fires in boreal, temperate, and tropical ecosystems: Parameters necessary to interpret historic fire regimes and future fire scenarios, *Sediment Records of Biomass Burning and Global Change* (J.S. Clark, H. Cachier, J.G. Goldammer, and B.J. Stocks, editors), NATO ASI Series, Subseries 1, “Global Environmental Change,” Vol. 51, Springer-Verlag, Berlin, Germany, pp. 169–188.
- Stocks, B.J., J.A. Mason, J.B. Todd, E.M. Bosch, B.M. Wotton, B.D. Amiro, M.D. Flannigan, K.G. Hirsch, K.A. Logan, D.L. Martell, and W.R. Skinner, 2002. Large forest fires in Canada, 1959–1997, *Journal of Geophysical Research—Atmosphere*, 108(D1:FFR5): 1–12.
- Van Wagner, C.E., 1977. Conditions for the start and spread of crown fire, *Canadian Journal of Forestry Research*, 7:23–34.

(Received 04 February 2003; accepted 11 March 2003; revised 06 May 2003)